

## FLUORIDE REMOVAL FROM AQUEOUS SOLUTIONS BY CUPRICOXIDE NANOPARTICLES

Edris Bazrafshan,<sup>a</sup> Davoud Balarak,<sup>a</sup> Ayat Hossein Panahi,<sup>a</sup> Hossein Kamani,<sup>a</sup>  
Amir Hossein Mahvi<sup>b,c,d</sup>  
Zahedan and Tehran, Iran

**ABSTRACT:** Excess fluoride ion (F) in drinking water causes harmful effects such as dental and skeletal fluorosis. Hence, its concentration in drinking water must not exceed a certain range. This study investigated the removal of F from aqueous solutions with CuO nanoparticles using a range of experimental approaches, including pH, adsorbent dose, contact times, and initial F concentration. The equilibrium adsorption data were analyzed using the Langmuir and Freundlich adsorption models. The maximum uptake value of F was 3152 mg/g at pH 5 during 40 min with 0.005 g/L nanoparticles of CuO and an initial F concentration of 5 mg/L. The fluoride adsorption equilibrium over the adsorbent was well described by the Freundlich model. The findings of this study showed that CuO nanoparticles are quite effective for F removal from aqueous environments. Thermodynamic analyses showed that the adsorption of F onto CuO nanoparticles was endothermic and spontaneous.

Key words: Adsorption; Cupric oxide nanoparticles; Fluoride removal

### INTRODUCTION

The fluoride ion (F) is classified as one of the contaminants of water for human consumption by the World Health Organization (WHO) and excessive ingestion can result in adverse health effects including dental and skeletal fluorosis.<sup>1</sup> Consequently, its concentration in drinking water must not exceed a certain range. According to the WHO standards, the permissible limit of F ions in drinking water is between 0.5 and 1.5 mg/L.<sup>2</sup> Groundwater is a major source of human intake of F. Besides the natural geological sources for F enrichment in groundwater, several industries are also contributing to F pollution to a great extent.<sup>3</sup>

Some industries which discharge wastewater containing high F concentrations include glass and ceramic production, electroplating, coal fired power stations, semiconductor manufacturing, brick and iron works, beryllium extraction plants, and aluminium smelters.<sup>4</sup> The discharges of these industries have higher F concentrations than natural waters, ranging from 10 to more than 1000 mg/L.<sup>5</sup> Furthermore, F is present in numerous environments such as groundwater,<sup>6,7</sup> bottled water,<sup>8,9</sup> and drinking water.<sup>10</sup>

Several processes are available at present for F removal both in the field and the lab, such as membrane filtration,<sup>11</sup> ion-exchange,<sup>12</sup> electrocoagulation,<sup>13</sup> and electrodialysis.<sup>14</sup> These methods, though being modernized, are still boring and time-consuming.<sup>15</sup> In contrast, the adsorption process, because of its simplicity, accessibility, convenience, cost effectiveness, and the availability of an extensive

---

<sup>a</sup>Health Promotion Research Center, Zahedan University of Medical Sciences, Zahedan, Iran; <sup>b</sup>School of Public Health, Tehran University of Medical Sciences, Tehran, Iran; <sup>c</sup>Center for Solid Waste Research, Institute for Environmental Research, Tehran University of Medical Sciences, Tehran, Iran; <sup>d</sup>For correspondence: Assistant Professor Amir Hossein Mahvi, Center for Solid Waste Research, Institute for Environmental Research, Tehran University of Medical Sciences, Tehran, Iran; Email: ahmahvi@yahoo.com.

range of adsorbents, is still one of the most extensively used processes. Many adsorbents, both natural and synthetic, have been successfully used for F removal including agricultural wastes,<sup>16</sup> carbon based materials,<sup>17</sup> activated alumina,<sup>18</sup> calcite,<sup>19</sup> granular ferric hydroxide,<sup>20</sup> and fly ash.<sup>21</sup> In the present work, CuO nanoparticles were utilized as nano adsorbents for the removal of F from aqueous solutions.

## MATERIALS AND METHODS

CuO nanoparticles (<100 nm) were purchased from Sigma-Aldrich (St. Louis, MO). The other chemicals used were analytical reagents (AR) grade. The standard stock F solution (1000 mg/L) used in this study was prepared by dissolving 0.221 g NaF into 1000 mL water. The stock solution was further diluted in order to prepare working solutions of the required concentration.

The adsorption experiments were carried out as batch tests in 250 mL flasks with magnetic stirring. Each test consisted of preparing a 100 mL of F solution with a desired initial concentration (5–100 mg/L) by diluting the stock F solution with distilled water, and transferring it into the beaker on the magnetic stirrer. The pH of the solution (3–13) was adjusted using 0.1N HCl or NaOH solutions. A known mass of CuO nanoparticles (0.003–0.1 g/L) was then added to the solution, and the obtained suspension was immediately stirred for a predefined time (5–120 min). After the desired contact time, the samples were withdrawn from the mixture by using a micropipette, the suspensions were centrifuged for 5 min at 6,000 rpm to remove the adsorbent, and the F concentration and the pH of the supernatant were analyzed. The concentration of the F remaining was measured using by the SPADNS method with a DR 5000 spectrophotometer (HACH Company, USA).

Adsorption kinetics were described by the pseudo first- and pseudo second-order models. In addition, equilibrium data were analysed by the Freundlich and Langmuir equilibrium isotherm models. In addition, thermodynamic parameters such as standard Gibbs free energy ( $\Delta G^0$ ), standard enthalpy ( $\Delta H^0$ ), and standard entropy ( $\Delta S^0$ ) were evaluated.

## RESULTS AND DISCUSSION

*Effect of initial pH on F adsorption:* The pH of the solution is an important factor controlling the surface charge of the adsorbent and the degree of ionization of the materials in the aqueous solution and is related to the  $pH_{pzc}$  (the pH point of zero charge) of the adsorbents. To determine the optimum pH for the maximum removal of F, the equilibrium sorption of F (with an initial F concentration of 20 mg/L) was investigated over the pH range of 3–13. As presented in Figure 1, it is obvious that the pH of the solution played a significant role on the adsorption of F onto the CuO nanoparticles. The adsorption amount of F on the CuO nanoparticles decreased with increasing initial pH, from 3144 and 3152 mg/g (at pH 3 and 5, respectively) to 2048 mg/g (at pH 13). In addition, the maximum removal efficiency of F was found to be 78.8% at pH 5.

At pH values lower than the  $pH_{pzc}$  of CuO nanoparticles ( $pH_{pzc}$  8.6), there is a high degree of attraction between positively charged CuO nanoparticles and negatively charged F, which can favor the adsorption of F onto CuO nanoparticles.

In contrast, at pH values higher than the  $pH_{pzc}$  of CuO nanoparticles, the adsorption of F onto CuO nanoparticles was restricted by the electrostatic repulsion between negatively charged CuO nanoparticles and negatively charged F, resulting in a low level of adsorption.<sup>22</sup> Similar findings have been reported by other researchers.<sup>23-25</sup>

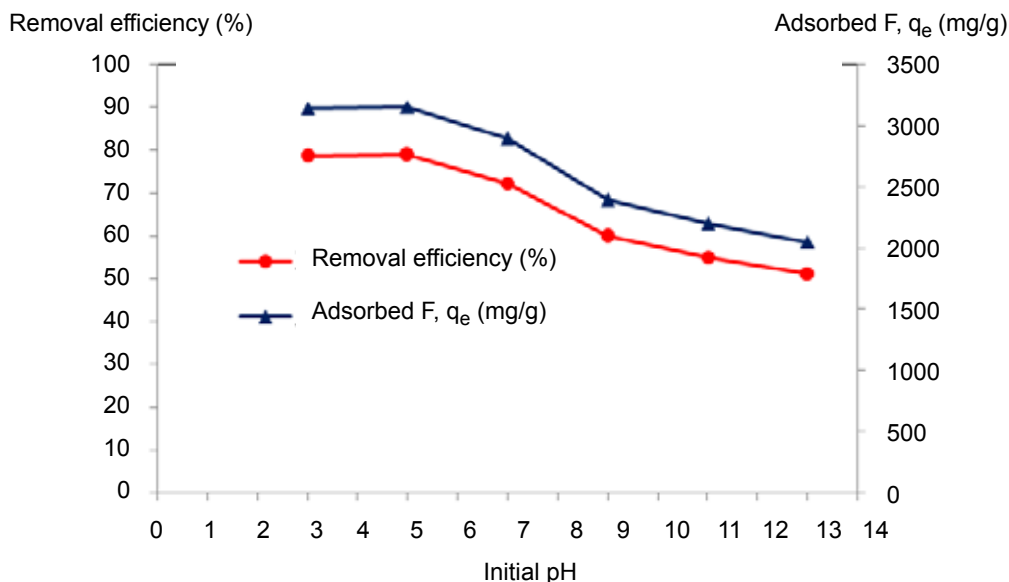


**Figure 1.** Effect of initial pH on F adsorption onto CuO nanoparticles (initial F concentration = 20 mg/L, adsorbent dosage = 5 mg/L, time = 40 min).

*Effect of CuO nanoparticles dose on F adsorption:* The adsorbent dosage is an important parameter because it determines the capacity of the adsorbent (CuO nanoparticles) for a given initial F concentration. Therefore, to evaluate the effect of adsorbent dose on the adsorption of F, 0.003–0.1 g/L CuO nanoparticles were used for adsorption experiments for 40 min at a fixed initial pH (pH 5), initial F concentration (20 mg/L), and temperature ( $22 \pm 1^\circ\text{C}$ ).

As presented in Figure 2, the adsorption capacity decreased from 4630 to 173 mg/g, while the removal percentage increased from 69 to 86.5%, when the CuO nanoparticles dosage increased from 0.003 to 0.1 g/L. The lower adsorption capacity of F at a greater dose of adsorbent is probably due to the decrease of the surface area of the adsorbent by the over lapping or aggregation during the sorption.<sup>26</sup> Nevertheless, the higher dose of the CuO nanoparticles in the solution and the greater the availability of active sites for F led to a higher removal of F. The maximum removal efficiency of F was observed with an adsorbent dose of 0.05 g/L. More F removal was not detected with a higher dosage of adsorbent and the removal continued approximately constant. Similarly, Bazrafshan et al. studied the effect of adsorbent dose (activated carbon obtained from cummin herb wastes) on the removal of Reactive Red-120 from aqueous solution.<sup>27</sup> Their findings

showed that the removal efficiency increased from 64 to 97%, while the  $q_e$  decreased from about 320 to 40 mg/g with an increase in the adsorbent dose from 0.1 to 1.4 g/L. Similar results have been reported by other researchers.<sup>28-31</sup>

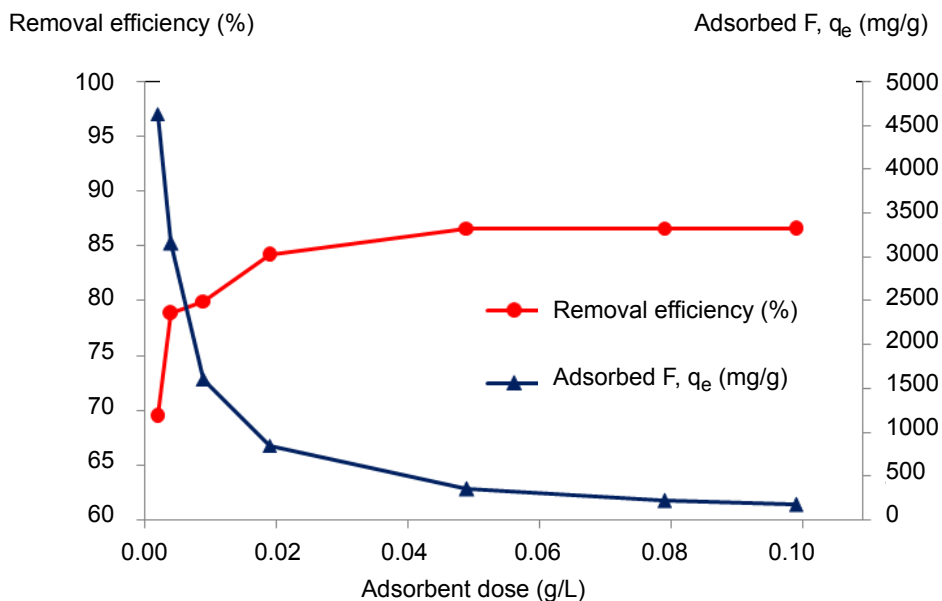


**Figure 2.** Effect of adsorbent dose on F adsorption onto CuO nanoparticles (initial F concentration = 20 mg/L, initial pH = 5, time = 40 min).

*Effect of contact time and initial F concentration:* The contact time between the pollutant and the adsorbent is one of the most important design parameters that affect the performance of adsorption processes.<sup>32</sup> The effect of contact time on the F adsorption by the CuO nanoparticles was investigated for 120 min at different initial F concentrations. As shown in the Figures 3 and 4, the amount of adsorbed F and the removal efficiency increased with prolonging the contact time and reached equilibrium at about 80 min for different initial concentrations. This indicates that the equilibrium time is independent of the initial fluoride concentration. Therefore, 80 min was selected as the optimum contact time for other experiments.

In fact, as shown in Figure 3 the removal of F increased with the increase in contact time at all initial F concentrations. For the first 60 min the adsorption uptake was rapid (~ 42–70%). It then proceeds at a slower adsorption rate and finally attains equilibrium at 80 min. Actually, a large number of vacant surface sites are available for adsorption during the initial stage, and, after a lapse of time, the remaining vacant surface sites are difficult to be occupied due to repulsive forces between the solute molecules on the solid and in the bulk phases.<sup>33</sup> Similar findings were reported by Cengizand and Cavas<sup>34</sup> and also by Gulnaz et al.<sup>35</sup>

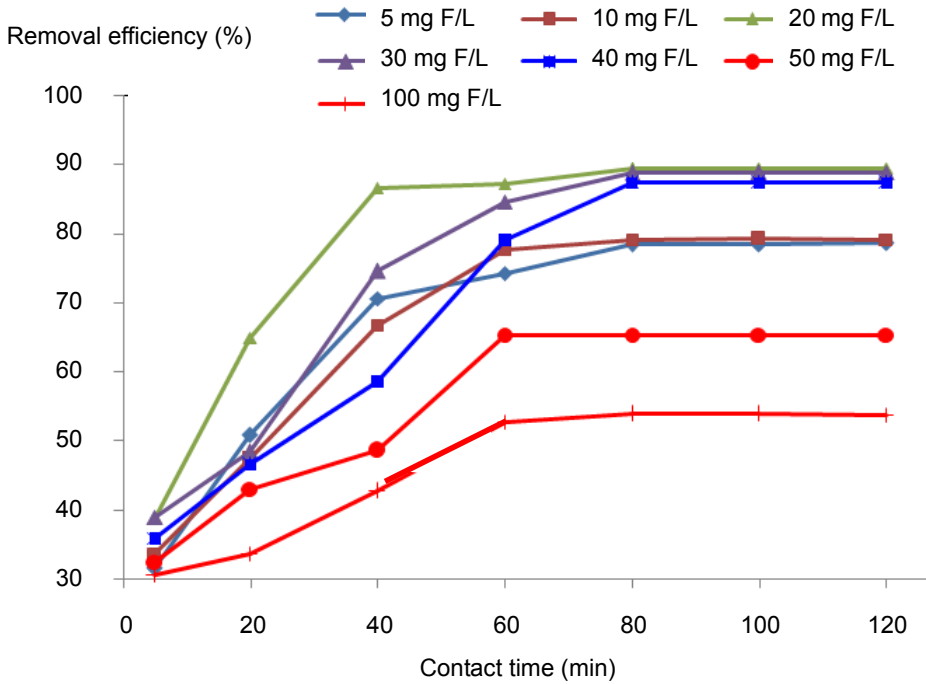


**Figure 3.** Effect of contact time for the adsorption of F onto CuO nanoparticles (trend of F removal).

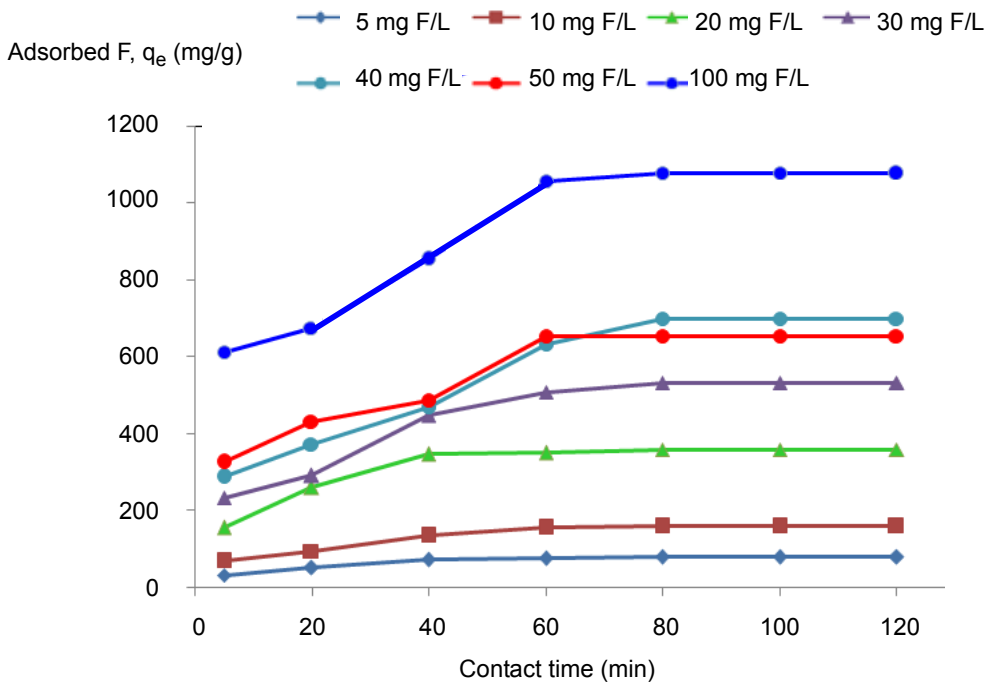


**Figure 4.** Effect of contact time for the adsorption of F onto CuO nanoparticles (trend of adsorbed F).

The effect of the initial concentration of F on the extent of adsorption by the CuO nanoparticles was studied and the relevant data are given in Figure 3. As can be seen, when the initial F concentration is increased, the percent of F removal decreased. In contrast, when the initial F concentration is increased, the amounts of adsorbed F also increase (Figure 4), so the removal of F depends on the concentration of the F in the solution. For example, when the initial concentration of F increases from 5 to 100 mg/L (at contact time 60 min), the equilibrium sorption capacities of CuO nanoparticles increase from 74.2 to 1056.2 mg/g. This increase in the proportion of removed F may be probably due to an equilibrium shift during the sorption process. In fact, the initial concentration of F provides an important driving force to overcome the mass transfer resistance of the F between the aqueous phases and the solid phases, so increasing the initial F concentrations would enhance the adsorption capacity of the CuO nanoparticles for F. In similar work, Mohammad et al. studied the effect of the initial F concentration on the adsorption of F by groundnut shell.<sup>36</sup> They observed that the F removal efficiency decreased from 93 to 82% with an increase in the initial F concentration from 5 to 30 mg/L.

*Effect of temperature on F adsorption and thermodynamic studies:* The effect of temperature on F adsorption was investigated at 293–313K. As it can be seen from Figure 5, the removal efficiency of F for all initial concentrations was increased, when the temperature was increased from 293 to 313K.

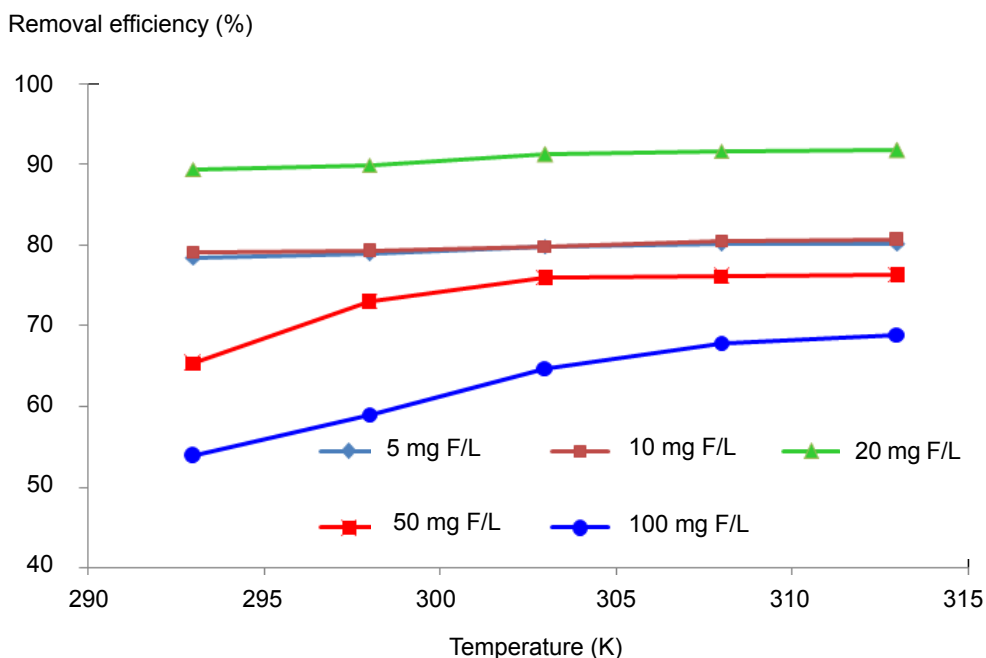


**Figure 5.** Effect of temperature on adsorption of F onto CuO nanoparticles (initial pH= 5, adsorbent dosage = 0.05 g/L, contact time= 80 min).

Increasing the temperature is known to increase the rate of diffusion of the adsorbate molecules across the external boundary layer and in the internal pores of the adsorbent particle, owing to the decrease in the viscosity of the solution.<sup>37</sup> Similar results have been reported by other researchers.<sup>25,38-40</sup>

In addition, to determine the thermodynamic parameters, experiments on F adsorption were carried out at different temperatures in the range 293–313K (kelvin). The free energy change ( $\Delta G^0$ ) of the sorption reaction is given as:

$$\Delta G^0 = -RT \ln K_a$$
$$\Delta G^0 = \Delta H^0 - T\Delta S^0$$

where R is the universal gas constant (8.314 J/mol/K) and T is the absolute temperature in K. The thermodynamic parameter, Gibb's free energy change,  $\Delta G^0$ , is calculated using  $K_a$  obtained from Freundlich and is shown in Table 3. The values of enthalpy ( $\Delta H^0$ ) and entropy change ( $\Delta S^0$ ) can be obtained from the slope of the plot of  $\Delta G^0$  versus T. A plot of Gibb's free energy change,  $\Delta G^0$ , against temperature, T, was found to be linear (Figure 6).

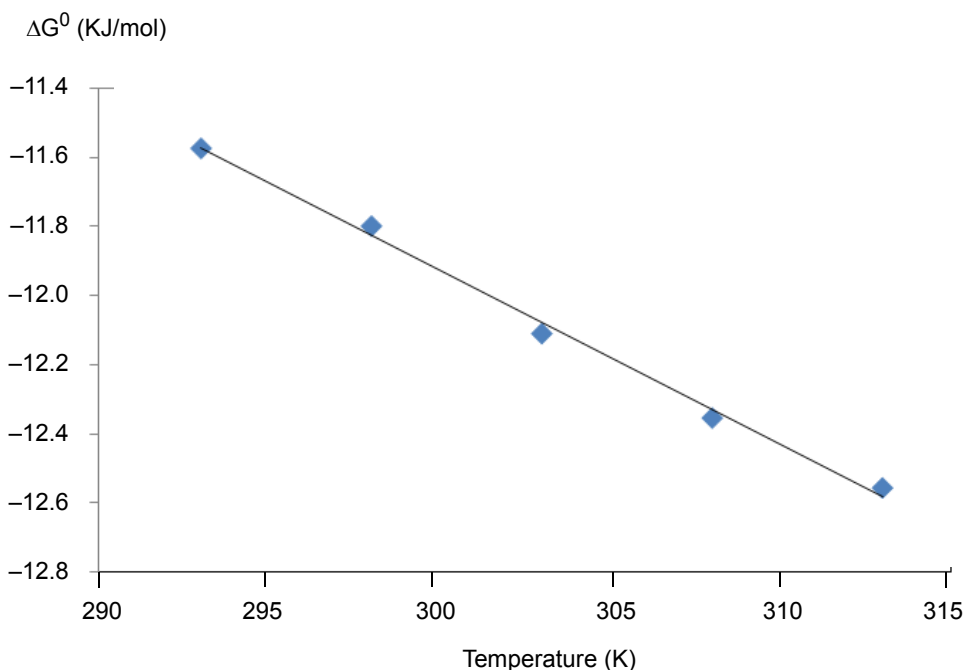


**Figure 6.** Plot of Gibbs free energy change,  $\Delta G^0$ , versus temperature, T.

The enthalpy change,  $\Delta H^0$ , and the entropy change,  $\Delta S^0$ , for the adsorption process were obtained from the intercept and slope of the above equation and found to be 3.22 kJ/mol and 0.05 kJ/mol/K, respectively. Also, the negative values of  $\Delta G^0$  confirm the feasibility of the process and the spontaneous nature of adsorption with a high preference of F by CuO nanoparticles. Additionally, the decrease in the negative value of  $\Delta G^0$  with an increase in temperature indicates

that the adsorption process of F on CuO nanoparticles becomes more favorable at higher temperatures.

The adsorption process can be categorized as physisorption and chemisorption by the magnitude of the enthalpy change. It is accepted that if extent of enthalpy change is less 84 kJ/mol, adsorption is physical. Nonetheless, chemisorption takes place in a range from 84 to 420 kJ/mol.<sup>41</sup> From these results (Table 1) it is clear that physisorption is much more favorable for F adsorption. Furthermore, the positive value of  $\Delta H^0$  indicates that the adsorption reaction is endothermic. Entropy has been defined as the degree of chaos of a system. Also, the positive values of entropy ( $\Delta S^0$ ) show the increased randomness of the solid-solution interface during the sorption of F on the CuO nanoparticles. These positive values of entropy may be due to some structural changes in the adsorbent during the adsorption process.

**Table 1.** Thermodynamic parameters for F adsorption on CuO nanoparticles

Temperature (K)	$\Delta G^0$ (kJ/mol)	$\Delta H^0$ (kJ/mol)	$\Delta S^0$ (kJ/mol K)
293	-11.57344705		
298	-11.79905228	3.22	0.05
303	-12.11046296		
308	-12.35530245		
313	-12.55796355		

*Kinetics of the adsorption process:* As illustrated in Figure 7, the removal rate of F by CuO nanoparticles was fast during the initial stages of the adsorption processes, especially for the initial F concentrations of 50 and 100 mg/L. However, the adsorption equilibrium was reached at 80 min for all the seven concentrations tested. The kinetic data in Figure 7 were treated with a pseudo-second-order rate equation. The second-order kinetic model is expressed as:

$$\frac{t}{q_t} = \frac{1}{K_2 q_e^2} + \frac{t}{q_e}$$

where  $k_2$  is the pseudo-second-order rate constant (g/mg/min);  $q_e$  the quantity of F adsorbed at equilibrium (mg/g);  $q_t$  the quantity of F adsorbed at time  $t$  (mg/g) and  $t$  is the time (min).

As it can be seen from Figure 7 the data fitted well with the second order kinetics model ( $R^2 > 0.99$ ). Also, the calculated  $q_e$  values agree very well with the experimental data (Table 2). Similar kinetic results have been reported in the adsorption of Reactive black 5 by multi-walled carbon nanotubes.<sup>25</sup>



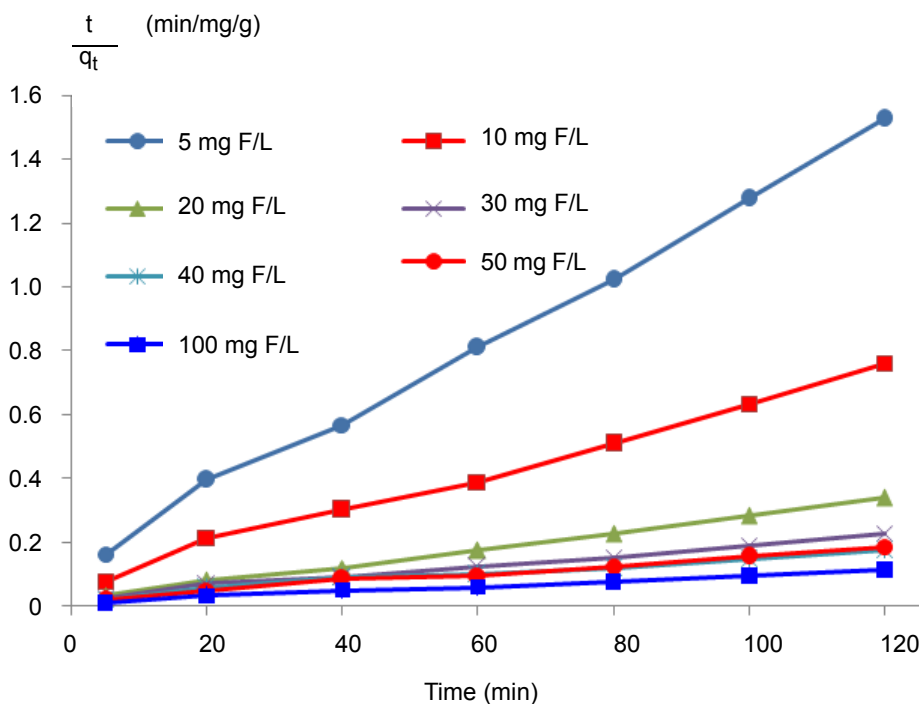


**Figure 7.** Pseudo-second-order kinetic plots for F adsorption on CuO nanoparticles at different initial concentrations of F (adsorbent dose = 0.05 g/L, pH 5, time = 5–120 min, and initial F concentration = 5–100 mg/L).

**Table 2.** Pseudo-second-order adsorption rate constants and  $q_e$  values for different initial F concentrations at pH 5

Initial F concentrations (mg/L)	$K_2$	$q_e$ (mg/g)	$R^2$
5	0.1175	0.0116	0.9976
10	0.0646	0.0057	0.9937
20	0.0127	0.0026	0.9982
30	0.0219	0.0017	0.9895
40	0.0228	0.0012	0.9752
50	0.015	0.0014	0.9878
100	0.0085	0.0008	0.9908

*Adsorption isotherms:* The interaction between the CuO nanoparticles as the adsorbent and F is clarified by the adsorption isotherm models. In the present study, two isotherms, namely the Langmuir and Freundlich isotherm models, were investigated. In fact, the isotherm provides a relationship between the concentration of the pollutant in solution and the amount of pollutant adsorbed on

the solid phase when both phases are in equilibrium.<sup>42</sup> According to the results of this study, the correlation coefficient of the Freundlich model, at 303–313K, was higher than that of the Langmuir model, indicating that the Freundlich model is suitable for describing the adsorption equilibrium of F onto CuO nanoparticles (Table 3). A similar result was reported by Bazrafshan et al. on methylene blue removal from aqueous solutions by low-cost ZnCl<sub>2</sub>-treated Pistachio-nut shell ash.<sup>43</sup>

**Table 3.** Isotherm parameters for adsorption of F onto CuO nanoparticles at various temperatures

		Langmuir isotherm				
Parameters	Temperature (kelvin)					
	293 K	298 K	303 K	308 K	313 K	
q <sub>m</sub> (mg/g)	20124.91	0.8927.69	6573.86	5858.18	5387.98	
k <sub>L</sub> (L/mg)	0.004	0.009	0.014	0.016	0.017	
R <sup>2</sup>	0.8539	0.8692	0.8307	0.8206	0.8156	
		Freundlich isotherm				
Parameters	Temperature (kelvin)					
	293 K	298 K	303 K	308 K	313 K	
k <sub>F</sub>	115.7	117.02	122.41	124.58	124.68	
n	1.65	1.51	1.43	1.40	1.38	
R <sup>2</sup>	0.8513	0.8586	0.8530	0.8567	0.8569	

### CONCLUSION

In the present study, the adsorption of F onto CuO nanoparticles was investigated. Batch adsorption tests demonstrated that the adsorption is affected by various conditions such as initial pH, adsorbent dosage, contact time, and initial F concentration. The findings show that CuO nanoparticles are an effective adsorbent for the removal of F from aqueous solutions. The equilibrium time was observed to be 80 min. A solution containing 20 mg F/L was treated at an efficiency of >89% where the removal capacity was 357 mg F/g CuO nanoparticles. The adsorption kinetics can be successfully fitted to the pseudo-second-order kinetic model. The equilibrium data for the adsorption of F on CuO nanoparticles were best represented by the Freundlich isotherm. The thermodynamic analyses showed that the adsorption of F onto CuO nanoparticles was endothermic and spontaneous. Furthermore, the adsorption of F onto CuO nanoparticles was via a physisorption process.

## ACKNOWLEDGMENTS

This study was funded by the Health Research Deputy of Zahedan University of Medical Sciences (Project No. 7425) and was conducted in the Chemical Laboratory of School of Public Health, Zahedan University of Medical Sciences.

## REFERENCES

- 1 Alagumuthlu G, Rajan M. Equilibrium and kinetics of adsorption of fluoride onto zirconium impregnated cashew nut shell carbon. *Chem Eng J* 2010;158:451-7.
- 2 WHO. Guidelines for drinking-water quality: incorporating first addendum to third edition. Vol 1. Recommendations. Geneva: World Health Organization; 2006. Available from: <http://helid.digicollection.org/en/p/printable.html>.
- 3 Reardon EJ, Wang Y. A limestone reactor for fluoride removal from wastewaters. *Environ Sci Technol* 2000;34:3247-53.
- 4 Shen F, Chen X, Gao P, Chen G. Electrochemical removal of fluoride ions from industrial wastewater. *Chem Eng Sci* 2003;58:987-93.
- 5 de la Puente G, Pis JJ, Menendez JA, Grange P. Thermal stability of oxygenated functions in activated carbons. *J Anal Appl Pyrolysis* 1997;43:125-38.
- 6 Dobaradaran S, Mahvi AH, Dehdashti S, Dobaradaran S, Shoara R. Correlation of fluoride with some inorganic constituents in groundwater of Dashtestan, Iran. *Fluoride* 2009;42(1):50-3.
- 7 Nouri J, Mahvi AH, Babaei AA, Ahmadpour E. Regional pattern distribution of groundwater fluoride in the Shush Aquifer of Khuzestan County, Iran. *Fluoride* 2006;39(4):321-5.
- 8 Fard RF, Mahvi AH, Hosseini SS, Khazaei M. Fluoride concentrations in bottled water available in Najaf and Karbala, Iraq. *Fluoride* 2014;47(3):249-52.
- 9 Dobaradaran S, Mahvi AH, Dehdashti S. Fluoride content of bottled drinking water available in Iran. *Fluoride* 2008;41(1):93-4.
- 10 Mahvi AH, Zazoli MA, Younecian M, Nicpour B, Babapour A. Survey of fluoride concentration in drinking water sources and prevalence of DMFT in 12 year old students in Behshahr City. *Journal of Medical Sciences* 2006;6:658-61.
- 11 Ndiaye PI, Moulin P, Dominguez L, Millet JC, Charbit F. Removal of fluoride from electronic industrial effluent by RO membrane separation. *Desalination* 2005;173:25-32.
- 12 Singh G, Kumar B, Sen PK, Majumdar J. Removal of fluoride from spent pot liner leachate using ion exchange. *Water Environ Res* 1999;71:36-42.
- 13 Bazrafshan E, Ownagh KA, Mahvi AH. Application of electrocoagulation process using Iron and Aluminum electrodes for fluoride removal from aqueous environment. *E-Journal of Chemistry* 2012;9(4):2297-08. [The journal name changed to *Journal of Chemistry* in 2013].
- 14 Amor Z, Bariou B, Mameri N, Taky M, Nicolas S, Elmidaoui A. Fluoride removal from brackish water by electrodialysis. *Desalination* 2001;133:215-23.
- 15 Gaoke Z, Zhili H, Xu W. A low-cost and high efficient zirconium-modified-Na-attapulgitite adsorbent for fluoride removal from aqueous solutions. *Chem Eng J* 2012;183:315-24.
- 16 Bazrafshan E, Khoshnamvand N, Mahvi AH. Fluoride removal from aqueous environments by ZnCl<sub>2</sub>-treated *Eucalyptus* leaves as a natural adsorbent. *Fluoride* 2015;48(4):315-20.
- 17 Mohan D, Singh KP, Singh VK. Wastewater treatment using low cost activated carbons derived from agricultural by products: a case study. *J Hazard Mater* 2008;152:1045-53.
- 18 Ghorai S, Pant KK. Investigations on the column performance of fluoride adsorption by activated alumina in a fixed-bed. *Chem Eng J* 2004;98:165-73.
- 19 Yang M, Hashimoto T, Hoshi N, Myoga H. Fluoride removal in a fixed bed packed with granular calcite. *Water Res* 1999;33:395-402.
- 20 Boldaji MR, Mahvi AH, Dobaradaran S, Hosseini SS. Evaluating the effectiveness of a hybrid sorbent resin in removing fluoride from water. *Int J Environ Sci Te* 2009;6(4):629-32.
- 21 Chaturvedi AK, Yadava KP, Pathak KC, Singh VN. Defluoridation of water by adsorption on fly ash. *Water Air Soil Pollut* 1990;49:51-61.
- 22 Miao L, Wang C, Hou J, Wang P, Ao Y, Dai S, Lv B. Effects of pH and natural organic matter (NOM) on the adsorptive removal of CuO nanoparticles by periphyton. *Environ Sci Pollut Res* 2015;22:7696-704.

- 23 Bazrafshan E, Kord Mostafapour F, Hosseini AR, Rakhsh Khorshid A, Mahvi AH. Decolorization of reactive red (120) dye by using single-walled carbon nanotubes in aqueous solutions. *Journal of Chemistry* 2013;2013: Article ID 938374; 8 pages; doi: 10.1155/2013/938374.
- 24 Zhanga G, Hea Z, Xu W. A low-cost and high efficient zirconium-modified-Na-attapulgite adsorbent for fluoride removal from aqueous solutions. *Chem Eng J* 2012;183:315-24.
- 25 Bazrafshan E, Kord Mostafapour F, Rahdar S, Mahvi AH. Equilibrium and thermodynamics studies for decolorization of Reactive Black 5 (RB5) by adsorption onto MWCNTs. *Desalination and Water Treatment* 2015;54(8):2241-51.
- 26 Kumar E, Bhatnagar A, Kumar U, Sillanpaa M. Defluoridation from aqueous solutions by nano-alumina: Characterization and sorption studies. *J Hazard Mater* 2011;186(2-3):1042-9.
- 27 Bazrafshan E, Ahmadabadi M, Mahvi AH. Reactive Red-120 removal by activated carbon obtained from cumin herb wastes. *Fresen Environ Bul* 2013;22(2a):584-90.
- 28 Tomar V, Prasad S, Kumar D. Adsorptive removal of fluoride from water samples using Zr-Mn composite material. *Microchemical Journal* 2013;111:116-24.
- 29 Bazrafshan E, Zarei AA, Nadi H, Zazouli MA. Adsorptive removal of Methyl Orange and Reactive Red 198 by *Moringaperegrina* ash. *Indian J Chem Techn* 2014;21:105-13.
- 30 Bazrafshan E, Kord Mostafapour F, Mahvi AH. Phenol removal from aqueous solutions using pistachio nut shell ash as a low cost adsorbent. *Fresen Environ Bul* 2012;21:2962-68.
- 31 Balarak D, Mahdavi Y, Bazrafshan E, Mahvi AH, Esfandyari Y. Adsorption of fluoride from aqueous solutions by carbon nano tubes: determination of equilibrium, kinetic, and thermodynamic parameters. *Fluoride* 2016;49(1):71-83.
- 32 Kord Mostafapour F, Bazrafshan E, Farzadkia M, Amini S. Arsenic removal from aqueous solutions by *Salvadora persica* stem ash. *Journal of Chemistry* 2013: Article ID 740847; 8 pages; doi:10.1155/2013/740847.
- 33 Kalavathy MH, Miranda LR. Comparison of copper adsorption from aqueous solution using modified and unmodified *Hevea brasiliensis* saw dust. *Desalination* 2010;255:165-74.
- 34 Cengiz S, Cavas L. Removal of methylene blue by invasive marine seaweed: *Caulerparacemosa var. cylindracea*. *Bioresource Technol* 2008;99:2357-63.
- 35 Gulnaz O, Sahnurova A, Kama S. Removal of Reactive Red 198 from aqueous solution by *Potamogetoncrispus*. *Chem Eng J* 2011;174:579-85.
- 36 Mohammad A, Majumder CB. Removal of Fluoride from synthetic waste water by using bio adsorbents. *International Journal of Research in Engineering and Technology* 2014;3(4):776-86.
- 37 Al-Qodah Z. Adsorption of dyes using shale oil ash. *Water Res* 2000;34:4295-303.
- 38 Bazrafshan E, Kord Mostafapour F, Alizadeh M, Farzadkia M. Dairy wastewater treatment by chemical coagulation and adsorption on modified dried activated sludge: a pilot-plant study. *Desalination and Water Treatment* 2016;57(18):8183-93.
- 39 Bazrafshan E, Alipour MR, Mahvi, AH. Textile wastewater treatment by application of combined chemical coagulation, electrocoagulation, and adsorption processes. *Desalination and Water Treatment* 2016;57(20):9203-15.
- 40 Bazrafshan E, Zarei AA, Kord Mostafapour F. Biosorption of cadmium from aqueous solutions by *Trichoderma* fungus: kinetic, thermodynamic, and equilibrium study. *Desalination and Water Treatment* 2016;57(31):14598-608.
- 41 Errais E, Duplay J, Darragi F, M'Rabetl, Aubert A, Huber F, Morvan G. Efficient anionic dye adsorption on natural untreated clay: Kinetic study and thermodynamic parameters. *Desalination* 2011;275:74-81.
- 42 Bazrafshan E, Kord Mostafapour F, Faridi H, Farzadkia M, Sargazi S, Sohrabi A. Adsorption of 2,4-dichlorophenoxyacetic acid (2,4-D) onto multi-walled carbon nanotubes. *Wulfenia* 2012;19(10):219-39.
- 43 Bazrafshan E, Mohammadi L, Kord Mostafapour F, Zazouli MA. Adsorption of methylene blue from aqueous solutions onto low-cost ZnCl<sub>2</sub> treated pistachio-nut shell ash. *Wulfenia* 2013;20(11 Pt 1):149-63.